ELSEVIER

Biochimica et Biophysica Acta 1278 (1996) 137–146

BBA Biochimica et Biophysica Acta

Cardiac Na$^+$ pump current–voltage relationships at various transmembrane gradients of the pumped cations

Helfried Günther Glitsch [a,*], Wolfgang Schwarz [b], André Tappe [a]

[a] Arbeitsgruppe Muskelphysiologie, Ruhr-Universität, D-44780 Bochum, Germany
[b] Max-Planck-Institut für Biophysik, Kennedyallee 70, D-60596 Frankfurt / Main, Germany

Received 12 July 1995; revised 14 September 1995; accepted 19 September 1995

Abstract

Thermodynamic considerations predict changes of the Na$^+$ pump current (I_p)–voltage (V) relationship of animal cells upon variations of the electrochemical gradients against which cations must be pumped. Experimental data in support of the predictions are sparse. Therefore, the effect on the I_p–V relationship of various electrochemical gradients for pumped Na$^+$ and Cs$^+$ was studied at constant ΔG_{ATP} (≈ -39 kJ/mol) in cardioballs from sheep Purkinje fibres. Control of the subsarcolemmal ionic concentrations during whole-cell recording was ensured by activation of I_p below its half maximal activity or by measuring the initial I_p following reactivation of the Na$^+$/K$^+$ pump. With gradients close to physiological conditions I_p was outward over the entire voltage range and the I_p–V relationship showed a maximum near zero potential. Steepening the ionic gradients diminished the I_p amplitude and outward pump current was no longer detectable between -65 mV and -110 mV. Flattened ionic gradients increased the I_p amplitude and shifted apparently the reversal potential E_{rev} to more negative values. These changes are in line with theoretical considerations. The measured I_p–V relationships were fitted by curves computed on the basis of a simplified Post-Albers scheme of Na$^+$/Cs$^+$ pumping. The increased I_p amplitude at flat ionic gradients was due to a decrease of [Cs$^+$]$_o$ for half maximal I_p activation. The maximal I_p amplitude remained unaffected.

Keywords: Whole-cell recording; Internal perfusion; Sodium ion depletion; Sodium pump current; Reversal potential; Ionic gradient; (Cardiac Purkinje cell)

1. Introduction

The Na$^+$/K$^+$ pump of animal cells extrudes 3 Na$^+$ from the cell and takes up 2 K$^+$ per each molecule of ATP hydrolysed. Thus, the electrical current produced by the activity of the Na$^+$/K$^+$ pump, the Na$^+$ pump current I_p, is an outward current under physiological conditions. The amplitude and voltage dependence of I_p are influenced by various factors. The activation of I_p by intra- and extracellular monovalent cations has been studied in several cells of different species and alterations of the cellular Na$^+$ pump current–voltage relationship (I_p–V relationship) by variations of the cation concentration have been described [4,23,25,26]. In addition it has been reported that simultaneous variation of the amount of free energy available from ATP hydrolysis (ΔG_{ATP}) and of the transmembrane gradients, against which the ions must be pumped, exerts a profound effect on the I_p–V curve. Under conditions, which decrease ΔG_{ATP} and simultaneously steepen the cation gradients, an inwardly directed I_p has been recorded [1,7,8]. Furthermore recent measurements on isolated, cultured cardiac Purkinje cells revealed a shift of the cardiac I_p–V relationship to the right and downwards to the V axis following a decrease of ΔG_{ATP} at constant sarcolemmal gradients of the pumped cations. As a consequence the reversal potential (E_{rev}) of I_p, i.e., the membrane potential where I_p is zero and reverses its direction, is moved into the range of membrane potentials, which is experimentally feasible [13]. While theoretical considerations predict that alterations of the transmembrane gradients of the pumped cations at constant ΔG_{ATP} will also affect the cardiac I_p–V relationship supporting experimental evidence is sparse. The experiments presented below address this point for the first time. The results lend support to the theoretical predictions. Some of the results have already been published in abstract form [12,31].

---

[*] Corresponding author. Fax: +49 234 7094129.

SSDI 0005-2736(95)00223-5

2. Methods

2.1. Preparation of single Purkinje cells

Single cells were isolated from sheep cardiac Purkinje fibres obtained from either ventricle at the local slaughterhouse. The isolation procedure has been described in detail before [10]. Briefly, the isolation was carried out at 37°C in a lamina flow cabinet. The fibres were superfused for about 100 min with Ca^{2+}-free Tyrode solution containing protease (0.2 mg/ml, type XXVII, P-4789; Sigma, St. Louis, MO, USA), collagenase (0.5 mg/ml, 1213865; Boehringer, Mannheim, Germany) and elastase (10 μl/ml, 20931; Serva, Heidelberg, Germany). Afterwards six different mixtures of a culture medium (Medium 199; Gibco, Paisley, UK) and of the Ca^{2+}-free Tyrode solution were subsequently applied for 20 min each to the fibres in order to increase stepwise the extracellular Ca^{2+} concentration. The culture medium was supplemented with 5% fetal calf serum (210463; Boehringer) and 1% Nutridoma-SR (1271091; Boehringer). The final superfusion fluid contained 50% culture medium and 50% Ca^{2+}-free Tyrode solution. Purkinje cells were squeezed out of the trimmed fibres into culture dishes (diam. 35 mm; Falcon, Becton Dickinson, Plymouth, UK) containing culture medium. The cells were cultured for up to 7 days at 95% humidity, 2% CO$_2$ and 37°C in an incubator (Heraeus B 5060 EK/CO$_2$; Hanau, Germany). Following 24 to 48 h in culture the cells exhibited a spherical shape (diam. between 40 and 70 μm; 'cardioballs', cf. [2]). The measurements were performed on cells cultured for 1 to 5 days.

2.2. Solutions

2.2.1. Control of the subsarcolemmal Na$^+$ concentration

The Na$^+$-containing pipette solution for intracellular perfusion was composed of (mM): 80 KCl, 40 KOH, 20 CsCl, 15 NaCl, 6 MgATP, 5 MgCl$_2$ (free [Mg^{2+}] $\approx$ 3.3 mM), 6 EGTA, 56 Hepes. In the Na$^+$-free pipette solution NaCl was replaced by KCl. The constituents of the Na$^+$-containing external bathing medium were (mM): 150 NaCl, 10.8 KCl, 1.5 MgCl$_2$, 0.9 CaCl$_2$, 2 BaCl$_2$, 5 NiCl$_2$ and 10 Hepes. Ba^{2+} and Ni^{2+} were added to diminish the K$^+$ and Ca^{2+} conductances of the sarcolemma and the sarcolemmal Na$^+$/Ca^{2+} exchange. The Na$^+$-free extracellular medium contained 150 mM choline chloride (plus $5 \cdot 10^{-6}$ M atropine sulfate) instead of 150 mM NaCl. The other constituents remained unchanged. In one experiment (Fig. 1B) Cs$^+$-containing solutions were applied. The composition of the pipette solution and the external media was the same as in series III (see below).

2.2.2. I_p–V curves at various sarcolemmal cationic gradients and constant ΔG_{ATP}

Variations of the gradients were achieved by changing the concentration of the intracellular (Cs$^+$) and extracellular (Na$^+$) main cation while keeping the concentration of the intracellular (30 mM Na$^+$) and external (20 mM Cs$^+$) activator cation of the Na$^+$/K$^+$ pump constant. Cs$^+$ was used as extracellular activator cation because it inhibits simultaneously the pacemaker current I_f [17], which might interfere with measurements of I_p at membrane potentials negative to ≈ -50 mV. In order to shift E_{rev} into a range of membrane potentials, which is experimentally feasible at steep ionic gradients, the concentrations of ATP, ADP and inorganic phosphate in the pipette solutions for internal perfusion were adjusted to obtain an internal ΔG_{ATP} of about -39 kJ/mol in each series of experiments. The details of the procedure were described elsewhere [13].

In *series I* intermediate sarcolemmal gradients, against which intracellular Na$^+$ (Na$_i^+$) and extracellular Cs$^+$ (Cs$_o^+$) must be pumped, were established. The pipette solution contained (mM; concentrations of the main intra- and extracellular cation in bold type): **60** CsCl, **50** CsOH, 20 NaCl, 10 NaOH, 10 MgATP, 20 TrisADP, **10** Cs$_2$HPO$_4$, **10** CsH$_2$PO$_4$, 3 MgCl$_2$ (free [Mg^{2+}] $\approx$ 0.4 mM), 6 EGTA, 36 Hepes. The composition of the external medium was (mM): **140** NaCl, **10** NaOH, 20 CsCl, 1.5 MgCl$_2$, 0.9 CaCl$_2$, 2 BaCl$_2$, 5 NiCl$_2$, 20 Hepes. The sarcolemmal gradients for the pumped Na$_i^+$ and Cs$_o^+$ were steepened in *series II*. The constituents of the pipette solution were (mM): **170** CsCl, **50** CsOH, 20 NaCl, 10 NaOH, 10 MgATP, 20 Tris-ADP, **10** Cs$_2$HPO$_4$, **10** CsH$_2$PO$_4$, 3 MgCl$_2$ (free [Mg^{2+}] $\approx$ 0.4 mM), 6 EGTA, 36 Hepes. The extracellular medium contained (mM): **240** NaCl, **10** NaOH, 20 CsCl, 1.5 MgCl$_2$, 0.9 CaCl$_2$, 2 BaCl$_2$, 5 NiCl$_2$, 20 Hepes. The transmembrane gradients, against which active Na$_i^+$ and Cs$_o^+$ transport has to occur, were lowered in *series III*. The pipette solution for intracellular perfusion was composed of (mM): **20** CsCl, 30 NaOH, 10 MgATP, 20 TrisADP, **10** Cs$_2$HPO$_4$, **10** CsH$_2$PO$_4$, 3 MgCl$_2$ (free [Mg^{2+}] $\approx$ 0.3 mM), 6 EGTA, 36 Hepes. The external medium had the following constituents (mM): **30** NaOH, 20 CsCl, 1.5 MgCl$_2$, 0.9 CaCl$_2$, 2 BaCl$_2$, 5 NiCl$_2$, 60 Hepes. The total concentrations of internal and extracellular Na$^+$ and Cs$^+$ used in series I–III are listed in Table 2.

The kinetics of I_p activation by Cs$_o^+$ were studied under the conditions of series I and III. However, the external media contained 40 mM (CsCl + TEACl). Variations of the extracellular Cs$^+$ concentration ([Cs$^+$]$_o$) were compensated by corresponding changes of the external [TEACl] in order to keep the concentration of CsCl plus TEACl constant at 40 mM.

The pH of all solutions mentioned above was adjusted to 7.4 by HCl or the hydroxide of the main cation.

2.3. Drugs

Dihydroouabain (DHO, No. 7197; Roth, Karlsruhe, Germany) was occasionally added to the external media from an aqueous stock solution (10^{-2} M) in order to identify I_p as current blocked by the cardiac glycoside. Cardiac glycosides are known to be specific blockers of the Na^+/K^+ pump [27].

2.4. Experimental procedure and whole-cell recording

A dish containing several hundred cardioballs was fixed at the stage of an inverted microscope (IM 35; Zeiss, Oberkochen, Germany) and a plastic ring was pushed down to the bottom of the culture dish in order to reduce its volume to ≈ 0.3 ml. The prewarmed (32–34°C) external solution was pumped into the dish at ≈ 0.6 ml/min and sucked off opposite to the inflow. The cell studied was superfused in addition by the external medium via a multibarrelled pipette (internal tip diam. ≈ 200 μm) near the cardioball. The solution was released from the pipette by gravitational force. The release was controlled by a command valve unit. Judging from variations in membrane current upon switching between media containing different $[K^+]$ the solution change was complete in less than 1 s.

Current (I)–voltage (V) curves were measured by means of whole-cell recording [14]. The initial resistance of the patch pipettes filled with one of the pipette solutions was between 1 and 3 MΩ. The pipettes were positioned at the sarcolemma by means of a micromanipulator (MO-103; Narishige, Tokyo, Japan). They were mounted on a holder as designed by Soejima and Noma [29] for intracellular perfusion with various media and modified as described elsewhere [10]. Voltage pulses were applied to the cardioball under study from a holding potential of -20 mV. The resulting membrane current was measured by means of an L/M EPC-7 patch clamp amplifier (List-Medical, Darmstadt, Germany). The current and the clamp potential were displayed on an oscilloscope (Tektronix 5111 A; Tektronix, Beaverton, OR, USA) and recorded by means of a penrecorder (R-50; Rikadenki Kogyo Co., Tokyo, Japan) or stored via an A/D converter (DT2801A; Data Translation; Marlborough, MA, USA) in a personal computer. The kinetics of I_p activation by Cs_o^+ were studied at holding potential. I_p was identified as current, which was activated by Cs_o^+ (or K_o^+) and blocked by DHO, a specific inhibitor of the Na^+/K^+ pump. Assuming a regular geometrical shape (cf. [10]) the surface of the cardioballs was estimated from the diameter measured through the microscope. Recording started 10–15 min after establishment of the whole-cell configuration to allow a sufficient exchange of the cytosol.

2.5. Statistics

Whenever possible data are shown as means ± S.E. As a rule S.E. is presented only if exceeding the size of the symbols in the figures. Differences between zero and mean values were checked by Student's one sample, two-tailed t-test. They were considered significant if $P \leq 0.05$. n represents the number of cells studied.

3. Results

3.1. Control of the subsarcolemmal Na^+ concentration

Whole-cell recordings from freshly isolated cardiac Purkinje and ventricular cells revealed variations of the subsarcolemmal Na^+ concentration upon abrupt changes of the Na^+/K^+ pump activity [3]. Thus, this technique does not guarantee per se an adequate control of subsarcolemmal ion concentrations under all experimental conditions. For experiments aimed at the effects of different sarcolemmal ionic gradients it is a prerequisite to ensure the existence of the intended gradients during whole-cell recording. Fig. 1A shows the activation of the Na^+ pump current I_p in a single cultured cardiac Purkinje cell by various extracellular K^+ concentrations ($[K^+]_o$) at the holding potential -20 mV. After a period of superfusion with a solution containing no activator ion of the Na^+/K^+ pump the cell is superfused with media containing various K^+ concentrations as indicated in the top trace of the figure. The bottom trace represents the membrane current. The outward shift of membrane current occurs following activation of the Na^+/K^+ pump and represents I_p [4]. Short pulses of K^+-free media indicate no variation of the membrane current in the absence of Na^+/K^+ pump activity. The various $[K^+]_o$ evoke an I_p, which declines from an initial peak to a lower steady-state value. This variation of the I_p amplitude is small with 1 mM K_o^+ and is more pronounced at higher $[K^+]_o$. Prolonging the period in K^+-free solution to more than 1.5 min affects neither the peak nor the steady-state I_p amplitude, whereas shortening reduces the peak I_p amplitude but leaves the steady-state value unaffected (data not shown). Reapplication of K^+-free medium shifts the membrane current in inward direction to the level observed prior to I_p activation. Repetitive short pulses of K^+-containing solution evoke an increasing I_p amplitude. Half maximal peak I_p was observed at 2.1 mM K_o^+, half maximal steady-state was measured at 1.4 mM K_o^+ ($n = 4$). Fig. 1B depicts a similar experiment where I_p is activated by various external Cs^+ concentrations ($[Cs^+]_o$) or a maximally effective concentration of K^+ (conditions of series III, see below). Changes between media without activator cations and solutions containing Cs_o^+ or K_o^+ are indicated by the upper trace. The lower trace displays the membrane current at holding potential. Cs_o^+ concentrations of ≤ 10 mM evoke an I_p with a constant amplitude. Higher concentrations of Cs_o^+ cause an I_p, which declines from an initial peak to a steady-state amplitude, similar to the activation of I_p by 10.8 mM K_o^+. Half maximum peak I_p activation by Cs_o^+ occurred at 8.5 mM Cs_o^+ ($K_{0.5}$ value) in this cell. Note that the decline of I_p is still small in the medium containing 20 mM Cs_o^+. Fig. 1C reveals that the occurrence of a peak I_p, which declines to a steady-state amplitude, is most probably due to subsarcolemmal Na^+ depletion during a strong Na^+/K^+ pump activation by external cations. A cardioball is internally

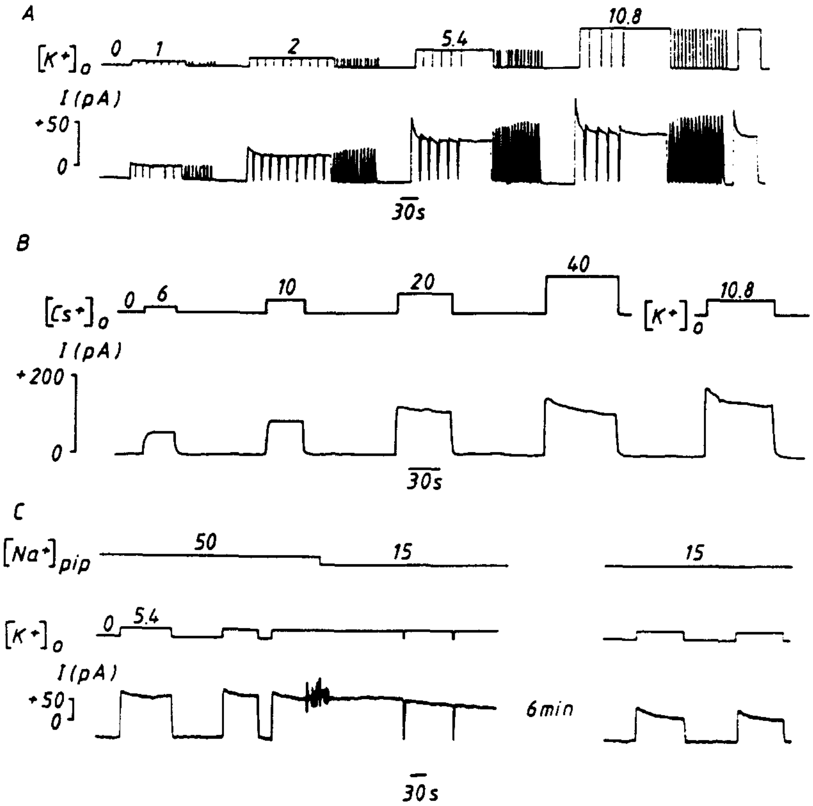

Fig. 1. Sample records from three cardioballs at the holding potential of −20 mV. (A) Activation of I_p by extracellular K^+. The upper line denotes variations of the extracellular K^+ concentration, the bottom trace displays the corresponding membrane current. (B) Activation of I_p by extracellular Cs^+. The Cs^+ concentrations applied are indicated above the current trace. Conditions of series III. (C) Effect of internal perfusion with pipette solutions containing different Na^+ concentrations. The variation of $[Na^+]_{pip}$ is shown by the top line. The middle line denotes variations of $[K^+]_o$. The bottom trace represents the corresponding membrane current. The noise on the current trace is caused by manual switching to the pipette solution containing 15 mM Na^+. In this and the following figures ionic concentrations are presented in mM.

perfused first with a pipette solution containing 50 mM Na^+ (Na^+_{pip}) and afterwards with a medium containing only 15 mM Na^+ (upper trace). I_p is activated by 5.4 mM K^+_o as shown by the middle trace. The bottom trace represents the membrane current at holding potential (−20 mV). I_p is nearly constant at higher $[Na^+]_{pip}$ during the Na^+/K^+ pump activation. A subsarcolemmal Na^+ depletion exerts less effect on I_p at high intracellular Na^+ concentrations than at lower Na^+ concentrations because I_p activation by $[Na^+]_{pip}$ exhibits saturation kinetics [10,23]. Thus, a decrease of the subsarcolemmal Na^+ concentration at high internal $[Na^+]$ does not diminish I_p since the Na^+-binding sites of the Na^+/K^+ pump remain saturated, whereas the same subsarcolemmal Na^+ depletion reduces I_p at lower intracellular $[Na^+]$ because Na^+-binding to the pump declines.

These data prompted the question whether experimental conditions exist, which permit a control of the subsarcolemmal Na^+ concentration by intracellular perfusion with pipette media or whether such control is impossible at all because the Na^+ influx across the sarcolemma determines the subsarcolemmal Na^+ concentration.

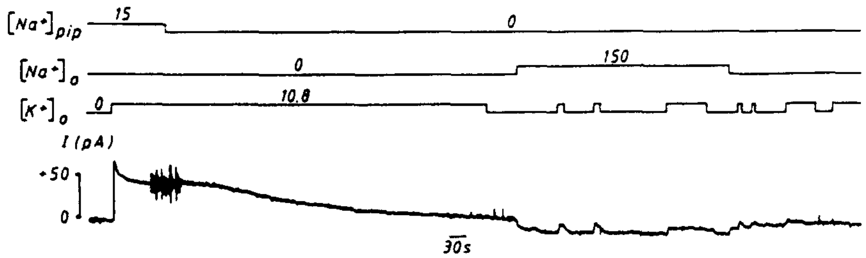

Fig. 2. Sample record from a cardioball. Changes of the Na^+ concentration of the pipette solution and of the Na^+ and K^+ concentration of the external medium are indicated by the upper three lines, the bottom trace displays the membrane current at a holding potential of −20 mV. The noise in the current trace is due to manual switching to the Na^+-free pipette solution.

In order to address this question measurements of I_p were carried out on cardioballs, to which intra- and extracellular media containing various Na^+ concentrations were applied. Fig. 2 presents an example. The upper three traces represent the Na^+ concentration of the pipette solution ($[Na^+]_{pip}$), the external Na^+ concentration ($[Na^+]_o$), and the extracellular K^+ concentration ($[K^+]_o$), respectively. The bottom trace displays the membrane current at holding potential (−20 mV). At the start of the record the cardioball is internally perfused with a pipette solution containing 15 mM Na^+ and superfused with a Na^+-free and K^+-free medium. Increasing $[K^+]_o$ to 10.8 mM activates I_p, which immediately peaks (≈ 70 pA) and declines afterwards towards a steady-state value. After a switch to a Na^+-free pipette medium I_p slowly decreases and vanishes after about 9 min when the membrane current is much the same in the presence or absence of K_o^+. Following application of a superfusion fluid containing 150 mM Na^+ at continued Na^+-free internal perfusion a small I_p (≈ 10 pA) can be reversibly activated upon an increase of $[K^+]_o$ to 10.8 mM. Reapplication of the Na^+-free external medium again abolishes I_p.

We conclude from the experiments illustrated in Figs. 1 and 2 that Na^+ influx through the sarcolemma is of minor importance for setting the actual subsarcolemmal Na^+ concentration. The concentration is mainly determined by the Na^+ influx from the pipette into the subsarcolemmal space and the Na^+ efflux from this space via the Na^+/K^+ pump. A reasonable control of the subsarcolemmal Na^+ concentration by intracellular perfusion seems feasible immediately after reactivation of the Na^+/K^+ pump when $[Na^+]$ beneath the sarcolemma is not yet lowered by Na^+ pumping or if the pumped Na^+ efflux does not exceed about 50% of the maximum active Na^+ efflux (Fig. 1A and B).

3.2. I_p–V relationships at different sarcolemmal ionic gradients and constant ΔG_{ATP}

Three series (I to III) of experiments were carried out at constant ΔG_{ATP} but different Na^+ and Cs^+ gradients. In each series the pipette solution for internal perfusion was composed to produce a ΔG_{ATP} of about −39 kJ/mol. The concentration of the pumped activator cations remained constant throughout ($[Na^+]_{pip}$: 30 mM; $[Cs^+]_o$: 20 mM). Different sarcolemmal Na^+ and Cs^+ gradients (see also Table 2) were established by various concentrations of the main intra- and extracellular cations (Cs^+_{pip}, Na^+_o).

Series I comprises experiments, in which external solutions containing 150 mM Na^+ and a pipette medium containing 140 mM Cs^+ were applied to the cardioballs. Fig. 3 displays an experiment of this series. The lower trace in part A represents the membrane current, the upper trace indicates the extracellular Cs^+ concentration. First the cell is superfused with Cs^+-free solution where I_p is absent. The small rectangular signal in the beginning of the current trace recorded during this period marks zero current level. Switching to an external medium containing 20 mM Cs^+ activates I_p and shifts the membrane current into the outward direction. Addition (bar above the trace) of the cardiac glycoside DHO, a specific inhibitor of the Na^+/K^+

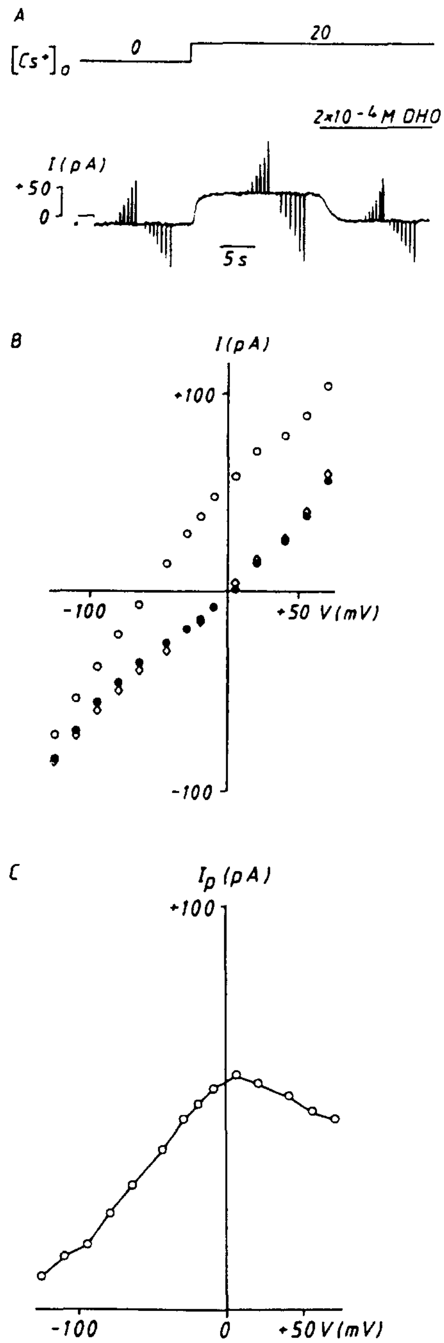

Fig. 3. I_p–V relationship of a cardioball. (A) Sample record from a cardioball at various $[Cs^+]_o$ (indicated by the top trace). The bottom trace presents the membrane current. Small rectangular signal indicates zero current level, vertical lines are due to voltage pulses applied from the holding potential of −20 mV. Experimental conditions of series I. (B) Current–voltage curves recorded in A in Cs^+-free medium (◇) and in Cs^+-containing solution with (●) or without DHO (○). (C) I_p–V relationship derived from the measurements in Cs^+-containing solution (○ minus ●). Line drawn to connect the data points.

pump, blocks I_p. The membrane current reaches the same level as in Cs^+-free solution. The vertical lines indicate three time intervals where I–V curves are taken by applying 200 ms voltage pulses to the cell at about 1 Hz from the holding potential of -20 mV. The resulting membrane current at the end of each clamp pulse is plotted versus clamp potential in Fig. 3B. The open diamonds represent the I–V relationship measured in Cs^+-free solution. Following I_p activation by 20 mM Cs_o^+ the I–V curve is shifted into the outward direction over the entire potential range studied (○). Addition of DHO to the external medium results in an I–V relationship (●), which superimposes on the curve measured in Cs^+-free solution since I_p is absent under both conditions. In order to derive the I_p–V curve the difference between corresponding membrane currents observed in Cs^+-containing solution with or without DHO is plotted versus membrane potential in Fig. 3C. I_p displays a maximum near zero potential and declines more strongly at negative than at positive membrane potentials. The pump current is outward over the entire range of membrane potentials studied.

Series II includes experiments where the sarcolemmal gradients, against which Na_i^+ and Cs_o^+ must be pumped, were steepened. For this purpose the medium for internal perfusion contained 250 mM Cs^+ and the external solution contained 250 mM Na^+ as the main cation. Fig. 4 shows an experiment on the cardioball, which exhibited the most positive E_{rev} of I_p and the strongest inward I_p at more negative potentials. The membrane current of the cardioball is measured at the holding potential (-20 mV) and is displayed in Fig. 4A. Application of DHO (right part of the trace) blocks I_p and shifts the current by ≈ 10 pA into the inward direction. The vertical deviations from the base line current represent the measurement of I–V relationships in DHO-free and DHO-containing medium, respectively. Voltage pulses of 500 ms duration are applied starting from the holding potential and the corresponding membrane currents are recorded. A close inspection reveals that the current is more inward in DHO-containing solution at positive clamp potentials, but is more outward at very negative voltages. The I–V curves measured in DHO-free (◇) and DHO-containing (♦) medium are plotted in Fig. 4B. They indicate a reversal of I_p at -45 mV. The reversal potential of I_p is more clearly seen in the I_p–V relationship depicted in Fig. 4C. I_p is outwardly directed at membrane potentials positive to -45 mV and is an inward current at more negative voltages. However, three other cardioballs examined in series II displayed I_p reversal potentials between -65 mV and -95 mV and I_p densities between -0.17 $\mu A\ cm^{-2}$ and -0.28 $\mu A\ cm^{-2}$ at -110 mV. Two additional cells showed positive I_p amplitudes over the entire range of membrane potentials tested. Their I_p densities amounted to $+0.06$ $\mu A\ cm^{-2}$ and $+0.12$ $\mu A\ cm^{-2}$ at -110 mV.

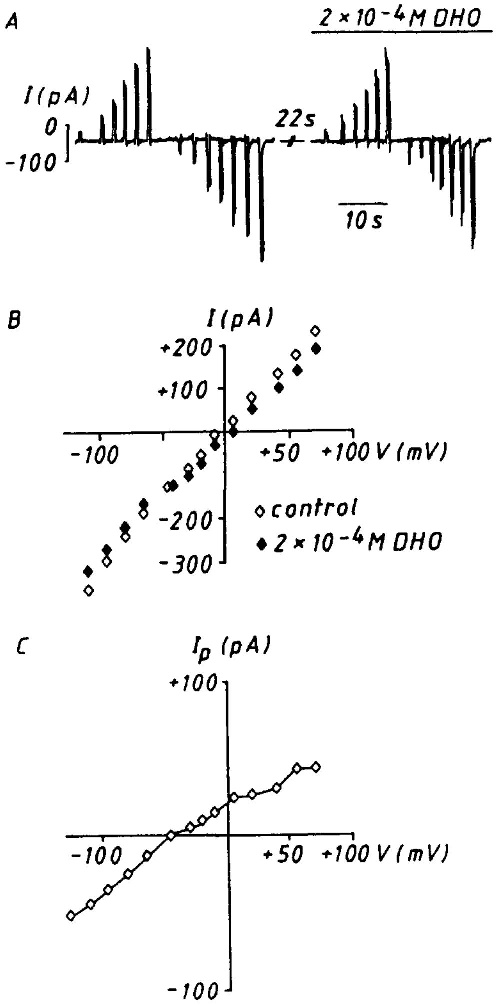

Fig. 4. I_p–V curve of a cardioball at steep ionic gradients (series II). (A) Sample record from a cultured Purkinje cell. Application of DHO is indicated above the right membrane current trace. The vertical deviations from the base line current are due to voltage pulses applied from the holding potential of -20 mV. (B) Current–voltage curves in Cs^+-containing external solution with (♦) or without DHO (◇) (from A). (C) I_p–V curve derived as difference from the I–V relationships depicted in B. Line drawn to connect the data points.

Normalized mean I_p–V relationships at constant ΔG_{ATP} and various sarcolemmal gradients of the transported Na and Cs ions are displayed in Fig. 5. The figure also includes the mean I_p–V dependency (▲) of the cardioballs studied in *series III* where the transmembrane gradients, against which Na_i^+ and Cs_o^+ must be pumped, are low ($[Na^+]_o$: 30 mM, $[Cs^+]_{pip}$: 50 mM). Each I_p–V relationship comprises the results from 6 cells. The I_p amplitudes observed at the various membrane potentials are first normalized to the corresponding I_p amplitude at $+5$ mV and then scaled with the respective mean I_p density at this potential (series I: ●, 0.41 ± 0.07 μA cm^{-2}; series II: ■, 0.32 ± 0.05 $\mu A\ cm^{-2}$; series III: ▲, 0.45 ± 0.12 $\mu A\ cm^{-2}$). Steepening the sarcolemmal gradients of the pumped cations shifts the I_p–V relationship towards the V axis and to the right. In each series I_p decreases with increasingly more negative membrane potentials. However, I_p reaches E_{rev} only in series II. The

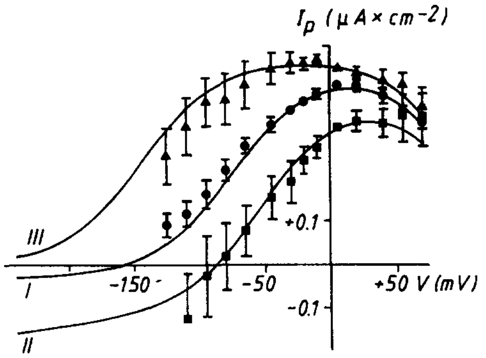

Fig. 5. Normalized $I_p - V$ relationships of cardioballs at different sarcolemmal Na^+ and Cs^+ gradients. ●, series I; ■, series II; ▲, series III. Each data point represents the mean of 6 cells. The curves represent fits to the data on the basis of a simplified Post-Albers scheme (Fig. 6), parameters are listed in Table 1. They cross the V axis at −88 mV, −159 mV and −340 mV, respectively.

two other I_p–V relationships suggest reversal potentials of I_p negative to the potentials, which are experimentally feasible. Thus E_{rev} seems to be shifted to more negative voltages with lower sarcolemmal gradients of the pumped Na^+ and Cs^+.

3.3. I_p–V curves derived by computer simulation

To describe the I_p–V relationship for the varying Na^+ and Cs^+ gradients (Fig. 5) we fitted an eight-step reaction scheme (see Fig. 6) based on the Post-Albers cycle to the data. Voltage dependence is assigned to the steps associated with extracellular Na^+ and Cs^+ binding (comp. [32]) and is described by voltage-dependent rates:

$$b_1 = b_1^* e^{-z_{Na} EF/RT} \tag{1}$$

$$f_2 = f_2^* e^{-z_{Cs} EF/RT} \tag{2}$$

E denotes the membrane potential. F, R and T have their usual meanings. z_{Na} and z_{Cs} represent apparent dielectric lengths of the access channel within the electric field for external Na^+ and Cs^+, respectively. Asterisks indicate the voltage-independent parts of the rate constants. Since two voltage-dependent steps are not sufficient to describe the complex voltage-dependence of pump activity, we arbitrarily assumed that external Na^+ deocclusion (f_8 in Fig. 6) represents an additional voltage-dependent step:

$$f_8 = f_8^* e^{z_{deocc} EF/RT} \tag{3}$$

Since one net charge is translocated across the entire membrane potential the z values have to obey:

$$z_{Na} - z_{Cs} + z_{deocc} = 1 \tag{4}$$

$z_{deocc} > 0$ means outward movement of a positive charge or inward movement of a negative charge during step f_8.

The 16 rate coefficients, f_i and b_i, are not independent but have to obey the principle of detailed balance:

$$\Psi = \frac{f_1 f_2 f_3 f_4 f_5 f_6 f_7 f_8}{b_1 b_2 b_3 b_4 b_5 b_6 b_7 b_8} = e^{-\Delta G_T / RT} \tag{5}$$

where

$$\Delta G_T = \alpha \Delta G_{ATP} + 3RT\left(\ln\frac{Na_o}{Na_i} - \frac{EF}{RT}\right) - 2RT\left(\ln\frac{Cs_o}{Cs_i} - \frac{EF}{RT}\right) \tag{6}$$

representing the change in total free energy. The free energy supplied by ATP hydrolysis is set to $\Delta G_{ATP} = -39$ kJ/mol, α was taken as an additional fit parameter and turned out to be close to one. The other two terms represent electro-chemical contributions due to the translocation of three Na and two Cs ions across the cell membrane, respectively. By applying the diagram method [16,19] and taking into account that one net charge (e^+) is transported across the cell membrane per pump cycle, the current I_p carried by N pump molecules can be written in the form:

$$I_p = \frac{Ne^+}{T}(f_1 f_2 f_3 f_4 f_5 f_6 f_7 f_8 - b_1 b_2 b_3 b_4 b_5 b_6 b_7 b_8) \tag{7}$$

T, in terms of the diagram method represents the sum of all directed trees. If I_p is expressed as current density (Fig. 5) N indicates the number of pump molecules per μm^2. As shown by Läuger [20], this can also be written in the form:

$$I_p = \frac{Ne^+}{\sum_{i=1}^{8} s_i}(\Psi - 1) \tag{8}$$

where

$$s_1 = (1 + K_2(1 + K_3(1 + K_4(1 + K_5(1 + K_6(1 + K_7(1 + K_8))))))))/b_1 \tag{9}$$

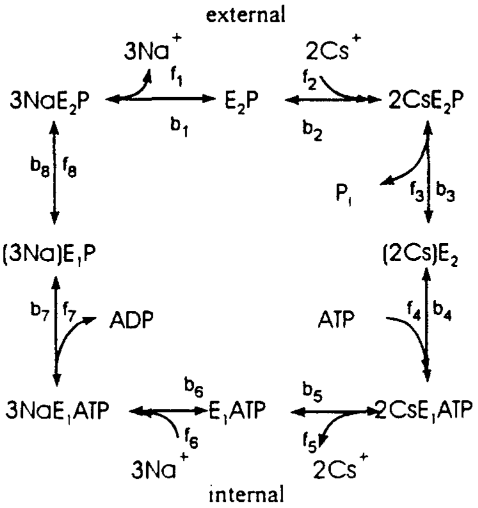

Fig. 6. Simplified, eight-step Post-Albers cycle of Na^+/Cs^+ pumping. The forward (f) and backward (b) rate constants of the partial reactions are indicated . E_1 and E_2 denote the two main conformational states of the Na^+/K^+ pump. (3Na) and (2Cs) refer to the occluded states of the ions.

Table 1
Numerical values of the fitted parameters in the simplified Post-Albers scheme (Fig. 6) of Na^+/Cs^+ pumping used for the computations according to Eq. (8)

Transition number	F	Constraint	B	Constraint	$K_{0.5}$ (mM)	h	Effective valence
1			$0.55\ s^{-1}\ mM^{-n}$	0.1–100	70	1.5	1.9
2	$10^3\ s^{-1}\ mM^{-n}$	$10–10^3$			1.7	**1.45**	1.0
3			$255\ s^{-1}\ mM^{-1}$	$1–5 \cdot 10^3$	0.47	**1**	
4	$10^6\ s^{-1}\ mM^{-1}$	$10^4–10^6$			0.3	**1**	
5			$1\ s^{-1}\ mM^{-1}$	$1–10^3$	37	**2**	
6	$10^3\ s^{-1}\ mM^{-n}$	10–1000			**9**	**1.53**	
7			$10^3\ s^{-1}\ mM^{-1}$	$1–10^3$	7.5	**1**	
8			$10^3\ s^{-1}$				0.1

The bold-printed parameters were kept constant and taken for external Cs^+ binding from Fig. 7 and for internal Na^+ binding from Ref. [10]. The rate coefficients F and B represent the voltage- and concentration-independent parts for the respective rates f_i and b_i. The values for N and α (see Eqs. (7) and (6)) were 560 μm^{-2} and 0.96, respectively. Constraints give the range of values the parameters were allowed to vary in the fit procedure. h represents the Hill coefficient.

$$s_2 = \big(1 + K_3\big(1 + K_4\big(1 + K_5\big(1 + K_6\big(1 + K_7\big(1 + K_8(1 + K_1)\big)\big)\big)\big)\big)\big)/b_2 \tag{10}$$

$$s_3 = \big(1 + K_4\big(1 + K_5\big(1 + K_6\big(1 + K_7\big(1 + K_8\big(1 + K_1(1 + K_2)\big)\big)\big)\big)\big)\big)/b_3 \tag{11}$$

$$s_4 = \big(1 + K_5\big(1 + K_6\big(1 + K_7\big(1 + K_8\big(1 + K_1\big(1 + K_2(1 + K_3)\big)\big)\big)\big)\big)\big)/b_4 \tag{12}$$

$$s_5 = \big(1 + K_6\big(1 + K_7\big(1 + K_8\big(1 + K_1\big(1 + K_2\big(1 + K_3(1 + K_4)\big)\big)\big)\big)\big)\big)/b_5 \tag{13}$$

$$s_6 = \big(1 + K_7\big(1 + K_8\big(1 + K_1\big(1 + K_2\big(1 + K_3\big(1 + K_4(1 + K_5)\big)\big)\big)\big)\big)\big)/b_6 \tag{14}$$

$$s_7 = \big(1 + K_8\big(1 + K_1\big(1 + K_2\big(1 + K_3\big(1 + K_4\big(1 + K_5(1 + K_6)\big)\big)\big)\big)\big)\big)/b_7 \tag{15}$$

$$s_8 = \big(1 + K_1\big(1 + K_2\big(1 + K_3\big(1 + K_4\big(1 + K_5\big(1 + K_6(1 + K_7)\big)\big)\big)\big)\big)\big)/b_8 \tag{16}$$

and

$$K_i = f_i/b_i \tag{17}$$

For the fitting, $K_{0.5}$ values and Hill coefficients were first assumed based on published values [20–22,30] and kept constant; one of the respective rate coefficients, f_i or b_i, was then fitted. Afterwards one to three of all parameters were fitted simultaneously in different combinations, and finally all parameters were fitted together to the data. The curves in Fig. 5 show the result of the fit and Table 1 lists the numerical values of the parameters used. Table 2 compares E_{rev} values for series I to III calculated according to Eq. (6).

Table 2
Concentration ratios and calculated reversal potentials for experiments of series I–III

Series	$[Na^+]_o/[Na^+]_i$ (mM/mM)	$[Cs^+]_o/[Cs^+]_i$ (mM/mM)	$E_{rev}^{\alpha\Delta G}$ (mV)
I	150/30	20/140	−159
II	250/30	20/250	−88
III	30/30	20/50	−340

$E_{rev}^{\alpha\Delta G}$ refers to $\alpha\Delta G_{ATP} = -0.96 \times 39$ kJ/mol.

3.4. Kinetics of I_p activation by Cs_o^+ at different Na^+ and Cs^+ gradients across the sarcolemma

Judging from Fig. 5 different sarcolemmal gradients (comp. Table 2) of the pumped Na and Cs ions vary the

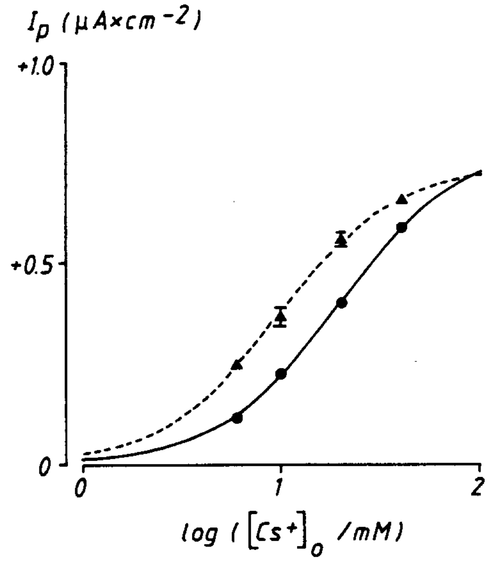

Fig. 7. I_p activation by Cs_o^+ at different sarcolemmal gradients of the transported cations. ●, series I; ▲, series III. The curves follow Eq. (18), with $K_{0.5} = 19.8$ mM (●) and $K_{0.5} = 9.9$ mM (▲). $n = 6$ and $h = 1.45$ for both curves.

amplitude of I_p. We studied possible differences in the I_p activation by Cs_o^+ on cardioballs under the experimental conditions of series I (●; $[Cs^+]_{pip}$: 140 mM, $[Na^+]_o$: 150 mM) and III (▲; $[Cs^+]_{pip}$: 50 mM, $[Na^+]_o$: 30 mM). The experiments were performed at the holding potential (−20 mV). Results from 6 cells in each series are depicted in Fig. 7. Normalized I_p densities are plotted as a function of the logarithm of $[Cs^+]_o$. The I_p amplitudes measured at the various $[Cs^+]_o$ are first normalized to the respective I_p amplitude recorded at 40 mM Cs_o^+ and then scaled with the I_p density observed at this $[Cs^+]_o$ (i.e. ●: 0.59 ± 0.12 $\mu A\ cm^{-2}$; ▲: 0.66 ± 0.18 $\mu A\ cm^{-2}$). The curves fitted to the data obey the Hill equation:

$$I_p = I_{p\,max}/1 + \left(\frac{K_{0.5}}{[Cs^+]_o}\right)^h \qquad (18)$$

where $I_{p\,max}$ denotes the maximum I_p density and $K_{0.5}$ stands for the $[Cs^+]_o$, at which I_p activation is half maximal. h represents the Hill coefficient and equals 1.45 in both series. Also $I_{p\,max}$ is nearly identical under both conditions (●: 0.80 $\mu A\ cm^{-2}$; ▲: 0.75 $\mu A\ cm^{-2}$). However, $K_{0.5}$ differs and amounts to 9.9 ± 1.06 mM under the conditions of series III (▲) and to 19.8 ± 1.1 mM under the conditions of series I (●).

4. Discussion

4.1. Measurement of I_p

In the experiments described above the Na^+ pump current was measured as current activated by external K^+ or Cs^+ and blocked by the cardiac glycoside DHO. Fig. 3A and B demonstrates that I_p is nearly the same regardless of whether it is defined as current activated by pump activator cations or as current inhibited by DHO. Both methods provided a reliable estimate of I_p over the entire range of membrane potentials studied. I_p was taken as an indicator for the activity of the Na^+/K^+ pump. This is correct only if the stoichiometry between the pumped Na^+ and K^+ fluxes remained unchanged under the present experimental conditions. So far a constant coupling ratio was observed following variation of ionic concentrations and membrane potential (see [6,28]) or in media containing cardioactive steroids [11]. To our knowledge no evidence exists for a direct regulation of the Na^+/K^+ pump by osmolarity or Cl^- concentration. Furthermore control experiments, in which the osmolarity was varied by addition of choline chloride to the intra- and extra-cellular media, showed no different I_p–V relationship (unpublished controls) and measurements with various Cl^- concentrations in the pipette solution for internal perfusion revealed no effect on I_p (cf. [15]). Therefore, it is unlikely that the results described above are due to changes in osmolarity and/or Cl^- concentration in series I to III.

4.2. Control of the subsarcolemmal Na^+ concentration

The introduction of the patch-clamp technique into electrophysiology rendered possible a better experimental control than hitherto of the media at both sides of the cell membrane. However, recent findings indicate that in the whole-cell mode of this technique an effective control of subsarcolemmal ionic concentrations, especially of Na^+, is not guaranteed under all experimental conditions (for a review see [5]). Figs. 1 and 2 show that this is true also in our experiments on single cultured Purkinje cells. A satisfactory control of the subsarcolemmal Na^+ concentration could be achieved initially after a period without Na^+/K^+ pump activity or during moderate activation of the Na^+/K^+ pump, when the diffusional exchange with the patch pipette solution determined the subsarcolemmal $[Na^+]$. The latter condition was chosen in the present experiments to study the voltage dependence of I_p at various ionic gradients across the sarcolemma. In each series (I to III) I_p was activated by 20 mM Cs_o^+. In series I half maximal I_p activation occurred at 19.8 mM Cs_o^+ and an even higher $K_{0.5}$ value has to be assumed for the experiments of series II. In series III the $K_{0.5}$ was lower than 20 mM (Fig. 7), but Fig. 1B demonstrates that under the conditions of series III the variation of the subsarcolemmal Na^+ concentration is still small. In the experiments aimed at the activation of I_p by Cs_o^+ the initial peak of the pump current after a period without Na^+/K^+ pump activity in Cs^+-free medium was taken as a measure of I_p. Thus, a reasonable control of the subsarcolemmal Na^+ concentration by internal dialysis existed during all experiments described above.

4.3. The I_p–V relationship of cardioballs varies with the sarcolemmal gradients of the transported cations

In order to study the effect of various transmembrane gradients of the pumped cations on the cardiac I_p–V curve, we carried out experiments at a constant ΔG_{ATP} but different ionic gradients, against which the ions must be pumped. In series I a conventional I_p–V relationship was recorded (see [4,23]). The curve displayed a positive slope at negative membrane potentials but only slight I_p variations at positive voltages. The I_p density differed from zero over the entire range of membrane potentials studied (Fig. 5). The I_p–V curve was shifted toward the V axis and to the right if the sarcolemmal gradients of the pumped ions were steepened (series II). The difference between the measured I_p densities and zero current level was insignificant at −65 mV to −110 mV suggesting the reversal potential of I_p to be within this range of membrane potentials. Similarly the computer simulation yielded a E_{rev} of −88 mV for the experiments of series II (Table 2). In this context it is appropriate to note that also the mean I_p density at −110 mV, the most negative membrane potential tested in series II (see Fig. 5), was statistically not different from zero, though 4 out of 6 cardioballs showed an inwardly directed I_p at this potential (see, for example, Fig. 4C). This is probably due to experimental shortcomings since the I_p densities within an appreciable range of membrane potentials near E_{rev} are known to be small and thus difficult to estimate, especially at low ΔG_{ATP} [13]. As in series I I_p in series III (diminished cationic gradients) differed significantly from zero current over the entire potential range tested. Clearly, a decrease of the sarcolemmal Na^+ and Cs^+ gradients shifted the I_p–V relationship upwards and to the left. Thus, the I_p density was increased throughout. E_{rev} seemed to be more negative than in the other two series. Thermodynamic considerations indeed predict a shift of E_{rev} into the negative direction with lowering the ionic gradients. The I_p–V curves derived by computer simulation provided a satisfactory fit to the data (curves in Fig. 5). E_{rev} values calculated for series I–III are listed in Table 2. A close inspection of Fig. 5 shows that the fit tends to get worse at the extreme voltages. This might indicate additional voltage-dependent partial reactions in the pump cycle apart from those included in the reaction scheme used for simulations (comp. Fig. 6 and Eqs. (1)–(3)). However, clear experimental evidence for such additional potential-dependent reactions is not available at present.

4.4. I_p increases with decreased sarcolemmal ionic gradients

A change of the sarcolemmal ionic gradients not only altered the voltage dependence of I_p, but also influenced the $K_{0.5}$ for I_p activation by Cs_o^+, whereas $I_{p\,max}$ remained unaffected. This is in contrast to the effect on the cardiac I_p–V curve of lowering ΔG_{ATP} at constant transmembrane gradients, against which Na^+ and Cs^+ must be pumped. Under those conditions $I_{p\,max}$ declined whereas the $K_{0.5}$ value remained unchanged [13]. A decrease of the ionic gradients, which was accompanied with a decrease of $[Na^+]_o$, lowered $K_{0.5}$ (Fig. 7) from 19.8 mM (series I) to 9.9 mM (series III). An interaction of external pump activator cations with Na_o^+ is known since the work of Post, Merritt, Kinsolving and Albright [24] and Garrahan and Glynn [9]. Recent papers confirmed a common binding site for these ions [18,32]. Our results are in line with a competitive antagonism between the cations with respect to the activation of the Na^+/K^+ pump.

However, the main result of the present paper is that at constant ΔG_{ATP} the cardiac I_p–V relationship varies with alterations of the sarcolemmal gradients of the pumped cations. The experimental data presented above are the first in support of the pertinent theoretical predictions.

References

[1] Bahinski, A., Nakao, M. and Gadsby, D.C. (1988) Proc. Natl. Acad. Sci. USA 85, 3412–3416.

[2] Bechem, M., Pott, L. and Rennebaum, H. (1983) Eur. J. Cell. Biol. 31, 366–369.

[3] Bielen, F.V., Glitsch, H.G. and Verdonck, F. (1991) Biochim. Biophys. Acta 1065, 269–271.

[4] Bielen, F.V., Glitsch, H.G. and Verdonck, F. (1991) J. Physiol. 442, 169–189.

[5] Carmeliet, E. (1992) Cardiovasc. Res. 26, 433–442.

[6] De Weer, P., Gadsby, D.C. and Rakowski, R.F. (1988) in The Na^+/K^+-pump. Part A: Molecular aspects (Skou, J.C., Nørby, J.G., Maunsbach, A.B. and Esmann, M., eds.), pp. 421–434, Alan R. Liss, New York.

[7] De Weer, P. and Rakowski, R.F. (1984) Nature 309, 450–452.

[8] Efthymiadis, A. and Schwarz, W. (1991) Biochim. Biophys. Acta 1068, 73–76.

[9] Garrahan, P.J. and Glynn, I.M. (1967) J. Physiol. 192, 175–188.

[10] Glitsch, H.G., Krahn, T. and Pusch, H. (1989) Pflügers Arch. 414, 52–58.

[11] Glitsch, H.G., Pusch, H. and Zylka, C. (1990) Naunyn-Schmiedeberg's Arch. Pharmacol. 342, 598–604.

[12] Glitsch, H.G. and Tappe, A. (1991) Pflügers Arch. 419, R105.

[13] Glitsch, H.G. and Tappe, A. (1995) J. Physiol. 484, 605–616.

[14] Hamill, O.P., Marty, A., Neher, E., Sakmann, B. and Sigworth, F.J. (1981) Pflügers Arch. 391, 85–100.

[15] Hermans, A.N., Glitsch, H.G. and Verdonck, F. (1994) J. Physiol. 481, 279–291.

[16] Hill, T.L. (1977) in Free Energy Transduction in Biology: The steady-state kinetic and thermodynamic formalism, Academic Press, New York.

[17] Isenberg, G. (1976) Pflügers Arch. 365, 99–106.

[18] Karlish, S.J.D., Goldshleger, R., Tal, D.M., Capasso, J.M., Hoving, S. and Stein, W.D. (1992) Acta Physiol. Scand. 146, 69–76.

[19] King, E.L. and Altman, C. (1956) J. Phys. Chem. 60, 1375–1378.

[20] Läuger, P. (1991) Electrogenic Ion Pumps, pp. 35–36, Sinauer Associates, Sunderland.

[21] Lemieux, D.R. and Kootsey, J.M. (1991) J. Theor. Biol. 150, 73–91.

[22] Liu, X.-Y., Kinard, T.A. and Stimers, J.R. (1992) Ann. N.Y. Acad. Sci. 671, 449–451.

[23] Nakao, M. and Gadsby, D.C. (1989) J. Gen. Physiol. 94, 539–565.

[24] Post, R.L., Merritt, C.R., Kinsolving, C.R. and Albright, C.D. (1960) J. Biol. Chem. 235, 1796–1802.

[25] Rakowski, R.F., Gadsby, D.C. and De Weer, P. (1989) J. Gen. Physiol. 93, 903–941.

[26] Rakowski, R.F., Vasilets, L.A., La Tona, J. and Schwarz, W. (1991) J. Membr. Biol. 121, 177–187.

[27] Schatzmann, H.-J. (1953) Helv. Physiol. Pharmacol. Acta 11, 346–354.

[28] Schwarz, W. and Vasilets, L.A. (1991) in The Sodium Pump: Structure, Mechanism and Regulation (De Weer, P. and Kaplan, J.H., eds.), pp. 327–338, Rockefeller University Press, New York.

[29] Soejima, M. and Noma, A. (1984) Pflügers Arch. 400, 424–431.

[30] Stimers, J.R., Liu, S. and Lieberman, M. (1991) J. Gen. Physiol. 98, 815–833.

[31] Tappe, A. and Glitsch, H.G. (1993) Proc. XXXII Congr. I.U.P.S. Glasgow, 48.11/P.

[32] Vasilets, L.A., Ohta, T., Noguchi, S., Kawamura, M. and Schwarz, W. (1993) Eur. Biophys. J. 21, 433–443.